The (Fe,Nb)Nb2Se10 family : resistivity and magnetic measurements

A. Ben Salem, A. Meerschaut, H. Salva, Z.Z. Wang, T. Sambongi

J. Physique **45** (1984) 771-778 AVRIL **1984**, PAGE 771

Classification
Physics Abstracts
72.15E — 71.30 — 75.20E

The (Fe,Nb)Nb_2Se_{10} family : resistivity and magnetic measurements

A. Ben Salem, A. Meerschaut

U.E.R. de Chimie, LA 279, 44072 Nantes Cedex, France

H. Salva, Z. Z. Wang

C.R.T.B.T.-CNRS, 38042 Grenoble Cedex, France

and T. Sambongi

Hokkaido University, Sapporo, Japan

(*Reçu le 19 juillet 1983, révisé le 14 novembre, accepté le 30 novembre 1983*)

Résumé. — Les propriétés physiques (électriques et magnétiques) des composés suivants : (FeNb)Nb_2Se_{10}, (Fe, V, Nb)Nb_2Se_{10}, (Cr, Nb)Nb_2Se_{10} et (Fe, Ta, Nb) (Nb, Ta)Se_{10} sont présentées et discutées en relation avec la structure. Ces quatre composés présentent une structure constituée de deux types de chaînes se développant à l'infini, parallèlement à l'axe *b* de la symétrie monoclinique (type structural de $FeNb_3Se_{10}$) : une chaîne trigonale prismatique $NbSe_3$ où se forme à basse température une onde de densité de charge (cas de (FeNb)Nb_2Se_{10}), et une chaîne octaédrique où règne le désordre dans la distribution des atomes métalliques. Ce désordre confiné uniquement sur la chaîne octaédrique semble être le facteur clé gouvernant les propriétés de transport. Il crée un potentiel aléatoire qui entraîne la localisation des électrons de conduction.

Abstract. — The physical properties (electric and magnetic) of (FeNb)Nb_2Se_{10}, (Fe, V, Nb)Nb_2Se_{10}, (Cr, Nb) Nb_2Se_{10} and (Fe, Ta, Nb) (Nb, Ta)Se_{10} are reported and a discussion is given in relation to their structural type. These four compounds exhibit two types of chains within the unit cell, running in a direction parallel to the monoclinic *b* axis ($FeNb_3Se_{10}$ structural type) : a trigonal prismatic chain ($NbSe_3$ like) where C.D.W.'s occurs at low temperature (as example $FeNb_3Se_{10}$), and an octahedral chain along which the disorder of the distribution of metallic atoms seems to be a key factor governing the transport properties; indeed, it creates a random potential causing the localization of the conduction electrons.

1. Introduction.

The existence of a new compound $FeNb_3Se_{10}$ was recently mentioned by Hillenius and Coleman [1]. The structural determination reported by Cava *et al.* [2] and Meerschaut *et al.* [3] indicated a similarity with the $NbSe_3$ structural type. The structure consists of two types of chains running parallel to the *b* axis. One is built from [$NbSe_6$] trigonal prisms sharing triangular faces the other is composed of edge-sharing [(Fe, Nb)Se_6] octahedra forming a double chain with disordered metal atoms.

The octahedral metal content seems to be able to present various Fe/Nb atomic ratios as was suggested by Whangbo *et al.* [4]; it was even formulated as $Fe_{1+x}Nb_{3-x}Se_{10}$ with $0.25 < x < 0.40$ excluding the previous $FeNb_3Se_{10}$ formulation. We did not try to vary the above atomic ratio but in this work we report structures and related physical properties of new materials involving various elements in the octahedral chain. Resistivity measurements suggest that the metal stoechiometry and/or atomic disorder within the octahedral chains are key factors governing the transport properties. Particularly, the resistivity rise which greatly differs for each compound of the family could be related to the characteristics of the octahedral chain.

2. Structural determinations.

2.1 In addition to the $FeNb_3Se_{10}$ compound, some related compounds were investigated by X-ray diffraction techniques. Unit cell parameters, chemical analyses and reliability factors are summarized

in table I for the already published results of (Fe, Nb)Nb_2Se_{10}(2, 3), (Cr, Nb)Nb_2Se_{10} and (Fe, V, Nb)Nb_2Se_{10} [5]. We attempted to prepare the tantalum derivatives MTa_3Se_{10} and MTa_3S_{10}(M = Fe, Cr...), as the binary tantalum trichalcogenides exhibit closely related structures with that of $NbSe_3$. We did not succeed in this way but, nevertheless, we obtained a new phase when starting from elements with the stoechiometric formula $FeTaNb_2Se_{10}$, which could primarily corresponds to the substitution for V by Ta in the octahedral chain.

A microanalysis of single needle-shaped crystals was made with a scanning electron microscope (microsonde Ouest-CNEXO) employing energy selection of the X-ray spectrum emitted by the specimen. Several areas were tested along the growing axis. Experimental and theoretical values are given in table II.

The unit cell parameters were refined by a least-squares method using powder data obtained from a Guinier-Nonius camera with $CuK\alpha_1$ radiation; $\lambda = 1.54051$ Å; silicon was used as an internal calibration standard :

$$a = 9.208(1)\text{ Å}, \quad b = 3.4856(5)\text{ Å},$$
$$c = 10.323(1)\text{ Å}, \quad \beta = 114.50(1)\text{ Å}$$

space group $P2_1/m$.

Table I. — (M, M') $(Nb_2)_{TP}Se_{10}$ *Unit cell parameters together with the chemical composition and reliability R factors.*

	$(Fe,Nb)_oNb_2Se_{10}$		$(Fe,V)Nb_2Se_{10}$	$(Cr,Nb)Nb_2Se_{10}$
	our work	Bell lab		
a (Å)	9.213 (1)	9.213 (1)	9.219 (1)	9.192 (2)
b (Å)	3.482 (1)	3.4773 (9)	3.4688 (5)	3.5086 (7)
c (Å)	10.292 (1)	10.299 (1)	10.223 (1)	10.409 (2)
β(°)	114.46 (4)	114.52 (1)	114.16 (1)	115.67 (1)
V (Å^3)	300.5	300.2	298.3	302.6
Chemical analysis (Microsonde OUEST-CNEXO)	$Fe_{1.2}Nb_{2.8}Se_{10}$	$Fe_{1+x}Nb_{3-x}Se_{10}$ $0.25 < x < 0.40$	$FeV_{0.5}Nb_{2.5}Se_{10}$	$Cr_{1.6}Nb_{2.4}Se_{10}$
Structural hypothesis	$(Fe,Nb)Nb_2Se_{10}$ R = 3.4 %	R = 4.1 %	$(FeV_{0.5}Nb_{0.5})Nb_2Se_{10}$ R = 3.3 %	$(Cr_{1.6}Nb_{0.4})Nb_2Se_{10}$ R = 8.9 %

Table II. — *Chemical analysis of the tantalum derivative (corrected weight fraction %).*

Experimental (four points on the same crystal)				Theoretical	
				$Fe_{1.3}Ta_{0.9}Nb_{1.8}Se_{10}$	$FeTaNb_2Se_{10}$
Fe	5.6	5.9	5.8 6.1	6.1	4.6
Ta	14.3	13.5	12.9 13.8	13.7	14.9
Nb	14.1	14.5	14.8 13.0	14.0	15.3
Se	66.1	65.9	66.5 67.1	66.2	65.1

A needle-shaped crystal with dimensions 0.01 × 0.02 × 0.77 mm^3 (the longest along the *b* axis) was used for the structural determination. 2 634 reflexions ($\pm h, +k, +l$) were measured in the range $2° < \theta < 42°$ using graphite monochromated $MoK\alpha$ radiation, with an ω-2 θ scan mode. After symmetry related reflexions were averaged and the reflexions having $I < 4\,\sigma(I)$ were rejected (calculations based on counting statistics), 1 089 independent reflexions remained for the structural analysis. Lorentz-polarization corrections were applied to the data. Absorption corrections ($\mu = 449$ cm^{-1}) were made for an idealized parallelepiped crystal shape; (between brackets are the distance (mm) from the crystal faces to an arbitrary origin inside the crystal); { 100 } (0.005), { 20$\bar{5}$ } (0.0$\bar{1}$), { $\bar{1}$00 } (0.05), { $\bar{2}$05 } (0.01), { 010 } (0.385), { 0$\bar{1}$0 } (0.385).

The structure was refined by the full matrix least-squares techniques with the assumption that $(FeTa)Nb_2Se_{10}$ and $(FeV)Nb_2Se_{10}$ are isostructural. Thus, in a first attempt, the Fe/Ta ratio was fixed equal to 1, the fractional coordinates and thermal parameters being coupled for both elements. A systematic series of refinements was then carried out in which the chemical composition was modified to take into account the results of the chemical analysis (particularly Fe/Ta ≠ 1). After many trials, the $Fe_{1.3}Ta_{0.9}Nb_{1.8}Se_{10}$ formulation gave the best reliability factor when assuming (Fe, Ta) in an octahedral coordination and (Nb, remaining Ta) in a trigonal prismatic coordination. At this stage, an anisotropic least-squares refinement led to the *R* values $R(F) = 0.048$ and $R_w(F) = 0.063$ but with very weak B_{eq} values attached to the (Nb, Ta) positions within the trigonal prismatic chain; $B_{eq}(\text{Nb, Ta})_{TP} = 0.31$ Å^2 opposed to $B_{eq}(\text{Fe, Ta})_{OCT} = 1.79$ Å^2. We then swapped the occupancy ratio within the trigonal prismatic chain, i.e. all the tantalum atoms being trigonally coordinated, that position being completed by niobium atoms. The B_{eq} values were inverted relative to the previous ones. An intermediate situation was then chosen. We supposed Ta atoms to be equally distributed in both types of sites (octahedral and trigonal prismatic). With such an hypothesis the refinement converged to the lower values $R(F)$: 0.028 and $R_w(F) = 0.044$. The two reflexions which were the most affected by the absorption correction, (020, 040) and a third one (141) were not in good agreement. Their rejection led to the final *R* values $R(F) = 0.025$ and $R_w(F) = 0.028$. The extinction parameter $g = 1.09 \times 10^{-6}$ was also refined. The final difference Fourier map was featureless.

The positional and thermal parameters are listed in table III; a list of the observed structure factors can be requested from the authors.

2.2 DISCUSSION. — Figure 1 shows the projection of the structure of the *XOZ* plane. The general features of this structure are the same as those of the $FeNb_3Se_{10}$ structural type. The interatomic distances,

Table III. — *Positional and thermal parameters and their estimated standard deviations.*

ATOM	OCCUP.	X	Y	Z	U(1,1)	U(2,2)	U(3,3)	U(1,3)
Ta O	22.5 %	0.4482(0)	3/4	0.0903(0)	0.0148(9)	0.017 (1)	0.0153(9)	0.0052(7)
Ta T	22.5 %	0.2752(0)	1/4	0.3638(0)	0.0084(3)	0.0058(4)	0.0092(3)	0.0034(3)
Nb T	77.5 %	0.2752(1)	1/4	0.3638(1)	0.0084(3)	0.0058(4)	0.0092(3)	0.0034(3)
Nb O	12.5 %	0.4482(0)	3/4	0.0903(0)	0.0148(9)	0.017 (1)	0.0153(9)	0.0052(7)
Se 1	100 %	0.4888(1)	3/4	0.3646(1)	0.0114(3)	0.0063(4)	0.0117(3)	0.0045(3)
Se 2	100 %	0.1615(1)	3/4	0.4921(1)	0.0162(4)	0.0075(4)	0.0163(3)	0.0085(3)
Se 3	100 %	0.0392(1)	3/4	0.2420(1)	0.0142(4)	0.0083(4)	0.0164(4)	0.0022(3)
Se 4	100 %	0.2414(1)	1/4	0.0899(1)	0.0182(4)	0.0122(5)	0.0124(4)	0.0059(3)
Se 5	100 %	0.6616(2)	1/4	0.1664(1)	0.0185(4)	0.0120(5)	0.0187(4)	0.0055(3)
FeO	65 %	0.4482(3)	3/4	0.0903(3)	0.0148(9)	0.017 (1)	0.0153(9)	0.0052(7)

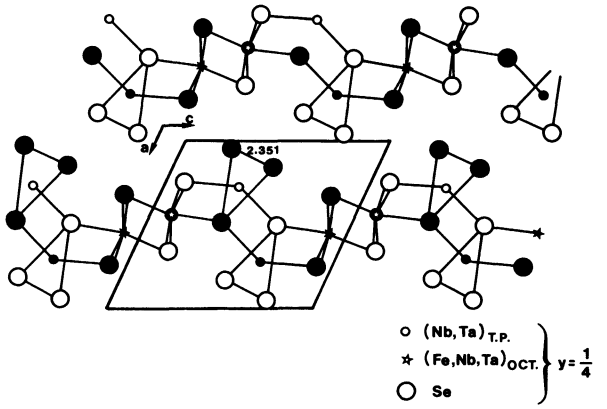

Fig. 1. — The structure of (Fe, Ta)Nb_2Se_{10} projected on to the *ac* plane.

table III, are very similar. The only differences consist in the occupancy of the octahedral and trigonal sites. This compound is the first example of this series to show an inhomogenous distribution of Nb and Ta atoms within the trigonal prismatic chains. The other compounds exhibit only pure [$NbSe_3$] trigonal prismatic chains.

3. Transport measurements.

3.1 We have measured the resistance of the (Fe, Nb)Nb_2Se_{10}, (Cr, Nb)Nb_2Se_{10}, (Fe, V, Nb) Nb_2Se_{10} and (Fe, Ta, Nb) (Nb, Ta)Se_{10} compounds with an ac bridge working at 33 Hz. The four contacts were either made of silver paint or obtained by pressure on gold strips evaporated on quartz substrates. When the resistance of the sample became higher than 1 MΩ we used a constant current source with a full scale range as low as 10^{-12} A. The measurement was then made only between both voltage leads. The connecting cable between the sample and the current generator was of triaxial type. The measure of the guard potential gave the resistance value. This technique allowed us to measure a calibrated resistance of 10^{10} Ω with an accuracy better than 0.5×10^{-3}. The anisotropy of (Fe, Ta, Nb) (Nb, Ta)Se_{10} was measured with the standard Montgomery method. The anisotropy within the *b-c* plane is not large. In the case of (Fe, Ta, Nb) (Nb, Ta)Se_{10} the room temperature value was found to be between 5 and 10 by repeated measurements with different samples.

In figure 2a, we have plotted Log R/R_0 *versus* Log T (R_0 : resistance of the sample at room temperature) for the four samples in the temperature range 1.5-300 K. Two remarks can be made :

i) These compounds undergo a metal-insulator transition at around the same temperature (T = 140 K) in agreement with the previous results of Hillenius *et al.* [6] for (Fe,-Nb)Nb_2Se_{10} although this

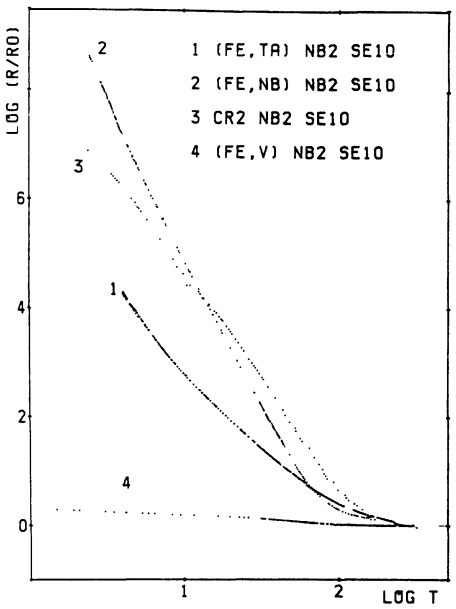

Fig. 2a. — Log of normalized resistance *versus* Log T for (Fe, Ta)Nb_2Se_{10}, (Fe, Nb)Nb_2Se_{10}, $Cr_2Nb_2Se_{10}$, (Fe, V)Nb_2Se_{10}.

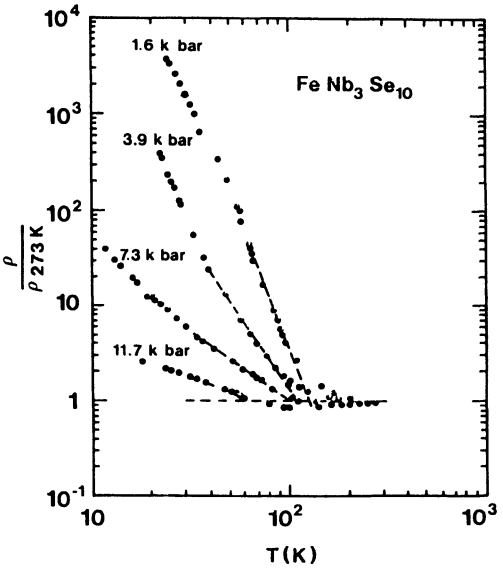

Fig. 2b. — Normalized resistivity of(Fe, Nb)Nb_2Se_{10} *versus* temperature for four pressures. After S. J. Hillenius and R. V. Coleman [1].

is not clearly demonstrated for the (Fe, Ta, Nb) (Nb, Ta)Se_{10} compound. In fact, as shown before, some disorder occurs in both types of chains (the trigonal chains are formed with tantalum and niobium atoms). Experiments are underway searching for evidence of a possible C.D.W. in this compound.

ii) The increase of the resistance is greatly different between these compounds. Thus, the resistance rise is about a factor of 10^9 for (Fe, Nb)Nb_2Se_{10} whereas it is only about 2 for (Fe, V, Nb)Nb_2Se_{10} in the same temperature range 140-2 K.

This second point may be indicative of a pressure like effect. Indeed, as most of these compounds differ only in regard to the octahedral chains, the result is that the *b* parameter reflects the metal-metal distances along both type of chains (octahedral and trigonal prismatic). Thus when replacing Nb (in octahedral coordination) by V in the $(FeNb)_0(Nb_2)_{TP}Se_{10}$ compound, one expects a metal-metal distance shorter than in the original material (3.482(1) Å for (Fe, Nb)Nb_2Se_{10} to be compared with 3.4688(5) Å) for (Fe, V, Nb)Nb_2Se_{10} and also a relative decrease of the Se-Se bondings between the chains in comparison with the decrease of the *C* parameter (10.299(1) Å → 10.233(1) Å respectively). As previously reported by Hillenius *et al.* (1), the resistivity of (Fe, Nb)Nb_2Se_{10} is found to be highly sensitive to pressure; under 12 kbar pressure, the rise in resistivity decreases from a factor of 10^9 to a factor 4 in the temperature range 140-3 K (Fig. 2b). At the same time, the onset temperature of the metal-insulator transition, T_p, decreases at a rate of 5 K.kbar^{-1}. The last feature is not found here since all these materials undergo a metal-insulator transition at roughly the same temperature (i.e. $T_p \sim 140$ K, see Fig. 3a for $FeVNb_2Se_{10}$ for example). We cannot say whether there could be a pressure effect as is observed for $FeNb_3Se_{10}$,

3.2 DISCUSSION. — Plotting $\log R/R_0$ *versus* $1/T$ between 300-4 K (Fig. 3a, b, c, d) we find that these four compounds do not behave as classical semiconductors. Below the transition temperature the variations of resistivity as a function of temperature cannot be described by a single exponential law over the whole temperature range. By contrast, the resistivity curves show various slopes indicating different conduction mechanisms. In these figures a very broad metal-insulator (M-I) transition is observed around $T \sim 140$ K, below which the resistivity increases as the temperature decreases. If we use the thermal activation relation, $\rho \propto \exp(\Delta E/2kT)$, to fit the experimental data, we may derive the values of E of the different compounds.

In mean-field theory the gap (2Δ) and the critical temperature T_c^{MF} are related by the B.C.S. relations,

$$T_c^{MF} = 0.57\,\Delta\,(T = 0)$$

for a quasi-one-dimensional system, the actual phase transition T_c should scale with the T_c^{MF} approximately as

$$T_c = \mu T_c^{MF}$$

where μ is a parameter, which depends on the transverse interaction and is thought to be about 0.25 or 0.4 [9, 10]. Combining above two relations, we have

$$T_c = \eta\Delta$$

where η is estimated to be between 0.14 and 0.23. It has been found for TTF-TCNQ, TaS_3 (monoclinic form), $(TaSe_4)_2I$ and $(NbSe_4)_{3.33}I$ that the values of η are 0.23, 0.18, 0.17 and 0.15 respectively [11]. Assuming $\Delta E = 2\Delta$, we find $\eta = 0.76$, 1.1, 0.56 and 10.66 for (Fe, Nb)Nb_2Se_{10}, (Fe, Ta, Nb) (Nb, Ta)Se_{10}, (Cr, Nb)Nb_2Se_{10} and (Fe, V, Nb)Nb_2Se_{10} respectively (cf. table V) all the values of η being greater than 0.23 (the (Fe, V, Nb)Nb_2Se_{10} compound differs from the others as the slope of resistivity curve is very small leading to a very small gap (0.2×10^{-2} eV)). It is evident that the simple Peierls transition which occurs in a quasi-one-dimensional system cannot explain the variation in conductivity of these compounds.

Such a situation suggests the correlation of the charge-density wave and the metal-insulator transition in these compounds as pointed out previously by Hillenius *et al.* [6].

An incommensurate structural distortion has been shown to occur for (Fe, Nb)Nb_2Se_{10} below ~ 140 K, with wave vector components **q** (0, 0.27, 0) [6]. Very recently, Moret *et al.* [7] observed a new X-ray diffuse scattering feature in (Fe, Nb)Nb_2Se_{10}. The intensity of this diffuse scattering increased slowly from room temperature down to about 150 K and then much faster below 150 K. They conclude that this new feature should be associated with the octahedral chains.

Table IV. — *Interatomic distances for each polyhedron* (Å).

M =Nb,Ta	- 2 Se 1 : 2.625	Se 1 - Se 2 : 3.756
	- 2 Se 2 : 2.654	Se 1 - Se 3 : 3.795
	- 2 Se 3 : 2.661	Se 2 - Se 3 : 2.351
	- 1 Se 1c : 2.743	
	- 1 Se 4 : 2.713	
M'= Fe,Nb,Ta	- 2 Se 4' : 2.580	Se 1 - Se 4 : 3.304
	- 2 Se 5c : 2.497	Se 1 - Se 5 : 3.529
	- 1 Se 1c : 2.698	Se 5c- Se 4 : 3.577
	- 1 Se 5 : 2.414	Se 5c- Se 5 : 3.902

Table V. — *Metal-insulator transition temperature and energy gap.*

	T_p (k)	ΔE (ev)	η
(Fe,Nb)Nb_2Se_{10}	137	0.030	0.76
(Fe,Ta,Nb)(Nb,Ta)Se_{10}	154	0.024	1.1
(Cr,Nb)Nb_2Se_{10}	140	0.043	0.56
(Fe,V,Nb)Nb_2Se_{10}	160	0.0025	10.66

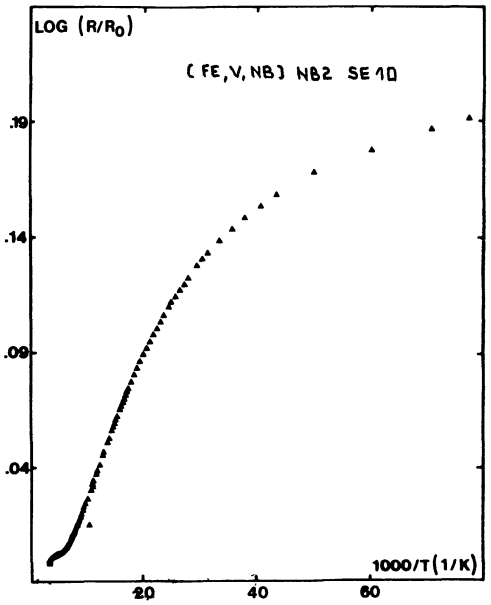

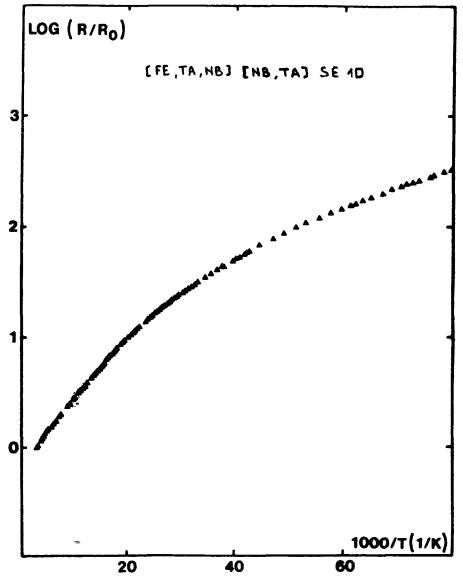

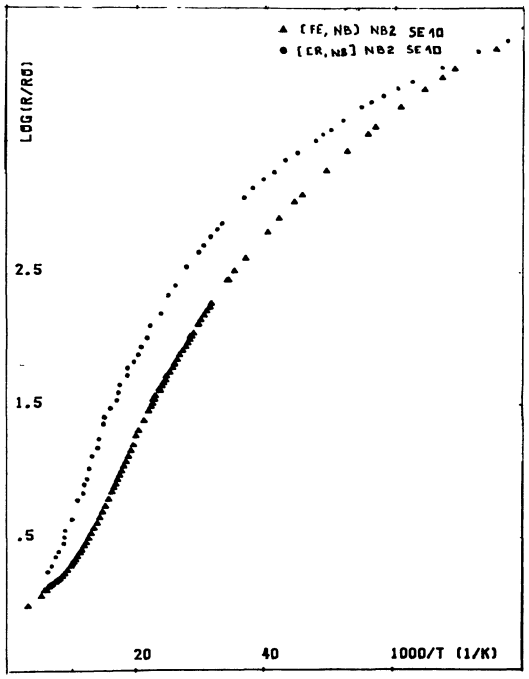

Fig. 3a. — Log of normalized resistance *versus* $10^3/T$ for (Fe, V)Nb_2Se_{10}, (Fe, Nb)Nb_2Se_{10}, $Cr_2Nb_2Se_{10}$, (Fe, Ta)Nb_2Se_{10}.

Based on the similarities with $NbSe_3$ it has been argued by Cava *et al.* [2] that the C.D.W. in (Fe, Nb)Nb_2Se_{10} lies on the [$NbSe_6$] trigonal prismatic chains.

Figure 4 shows the variations of Ln ρ/ρ_0 as a function of $\left(\frac{1}{T}\right)^{1/4}$ at low temperatures (for (Fe, Nb)Nb_2Se_{10}, (Fe, Ta, Nb) (Nb, Ta)Se_{10} and (Cr, Nb)Nb_2Se_{10} and figure 5 shows that of (Fe, V, Nb)Nb_2Se_{10}). In the range 40 K-4 K, the data are well fitted with a function of the form $\rho \propto \exp T^{-1/4}$, as shown by the straight lines portions. This is characteristic of a thermally activated hopping mechanism.

In disordered solids with a narrow conduction band of width B, a narrow potential V is included in the lattice potential V_0. If the inequality $| V | < 1/2 | V_0 |$ is obeyed and V_0/B is greater than a certain critical value, all electron states below « the mobility edge » E_c will be localized in space. When the difference between the Fermi energy E_F and E_c changes sign, a metal-insulator transition (Anderson transition) occurs [12]. In the localized state two forms of conduction are possible, and in general take place in parallel : *a*) thermal excitation of electrons where $\sigma_{ext} = \sigma_{min} \exp \{ -(E_c - E_F)/kT \}$ with $(\sigma_{min})^{-1}$ estimated between 3 and 15 mΩ.cm for (FeNb)Nb_2Se_{10} family, and *b*) by electron hopping between nearest localized states where $\sigma_{hopp} = \sigma_0 \exp -\left[\frac{T_0}{T}\right]^{1/4}$.

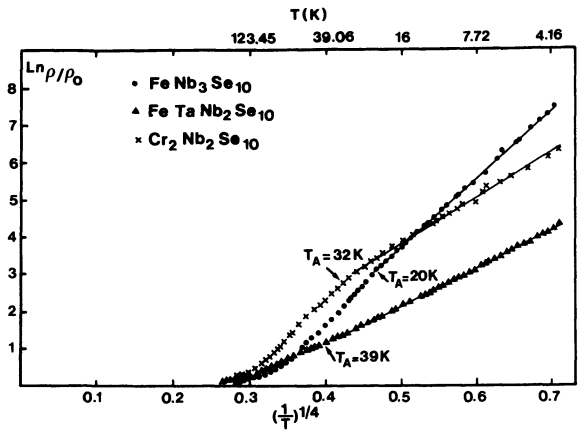

Fig. 4. — Log of normalized resistivity *versus* $T^{-1/4}$ for (Fe, Ta)Nb_2Se_{10}, (Fe, Nb)Nb_2Se_{10}, $Cr_2Nb_2Se_{10}$.

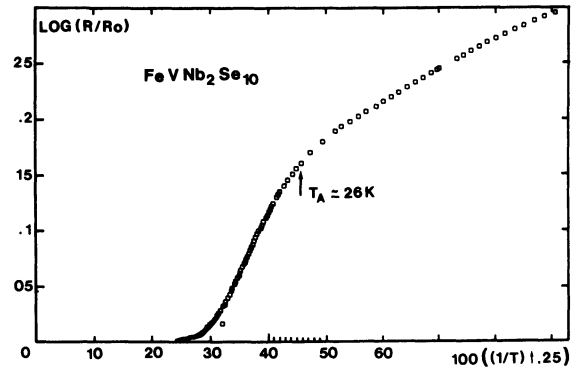

Fig. 5. — Log of normalized resistance *versus* $100.T^{-1/4}$ for (Fe, V)Nb_2Se_{10}.

In (FeNb)Nb_2Se_{10} family the atoms Fe, V, Cr are randomly distributed in the octahedral chains. The random potential dominates in one set of metal chains in which an Anderson transition take place at some temperature (certainly for $T \gg 30$ K, perhaps $\sim$ 200 K ?), and so the resistivity rise is partly due to Anderson localization.

The coexistence of the C.D.W. and Anderson localization is a result of the crystal structure of these compounds. We have two types of conduction chains in these compounds, pure Nb chains and Fe (or V, Cr) Nb mixed chains, and we can assume that the conductivity of the compounds arises from these two parts. Before the C.D.W. formation, the pure Nb chains are considered as good conductors with a conductivity σ_{pure} (T = 290 K) $\sim$ ($\eta \times 300$ μΩcm)$^{-1}$ similar to that in $NbSe_3$. As a result of the random potential the conductivity of the mixed chains σ_{mix} is much smaller than that of the pure Nb chains at temperatures above 100 K. Below the C.D.W. transition temperature, localization on the pure trigonal niobium chains is favorable because of the following two mechanisms.

The decrease of electronic density of states due to the C.D.W. formation and the randomly distributed atoms in octahedral chains.

In this model the activation energy deduced from the resistivity measurements is not the Peierls gap but the difference between E_F and the mobility edge E_C. The fact that the slope of the curves log ρ *vs.* $(1/T)$ tends towards zero, which is the signature of Anderson localization, means that ρ becomes nearly constant. We then plotted the quantity $\Delta\sigma$, $(1/\rho_0 - 1/\rho)$, as a function of Ln T for all these compounds (Fig. 6). $\Delta\sigma$ is constant below a threshold temperature (which differs for each compound) as verified for (Fe, Nb)Nb_2Se_{10}, (Fe, Ta, Nb) (Nb, Ta)Se_{10} and (Cr, Nb)Nb_2Se_{10}, thus indicating strong localization. However, $\Delta\sigma$ is not constant for the (Fe, V, Nb)Nb_2Se_{10} compound, but it shows a linear variation which reveals, in that case, weak localization.

4. Magnetic measurements.

Magnetic susceptibility of (Fe, Ta, Nb) (Nb, Ta)Se_{10} and (Fe, V, Nb)Nb_2Se_{10} was measured with a Faraday balance system (resolution of 1 μg) in the temperature range between 300 and 4.2 K. Samples were selected from agglomerates of fibre-shaped crystals under a microscope to avoid contamination with unreacted material. About 0.02 g was used for each measurement. The measured susceptibility was found to be independent of the magnetic field strength below 7.8 kOe down to the lowest temperature. Samples which showed field-dependent susceptibility at room. temperature were discarded. The susceptibility of (Fe, Nb)Nb_2Se_{10} has been measured by Hillenius *et al.* [6].

Figures 7, 8 show the magnetic susceptibilities *versus* temperature for (Fe, V, Nb)Nb_2Se_{10} and (Fe, Ta, Nb) (Nb, Ta)Se_{10}. Both curves exhibit the same characteristics as the previously reported ones of (Fe, Nb)Nb_2Se_{10} [6]. The magnetic susceptibilities which are nearly constant between 300-200 K show a minimum at around 200 K and then rise rapidly at lower temperatures. The constant part is attributed to

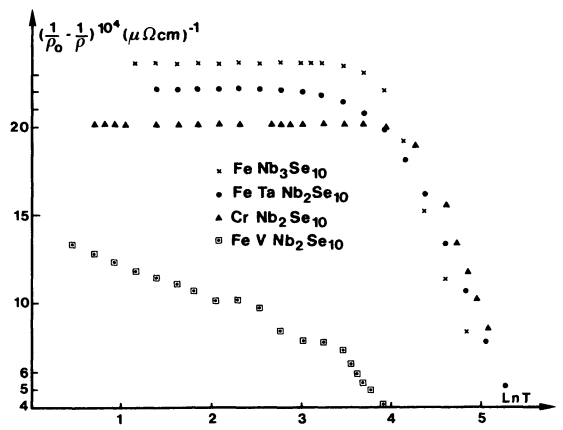

Fig. 6. — $(1/\rho_0 - 1/\rho)$ *versus* Ln T for our four compounds.

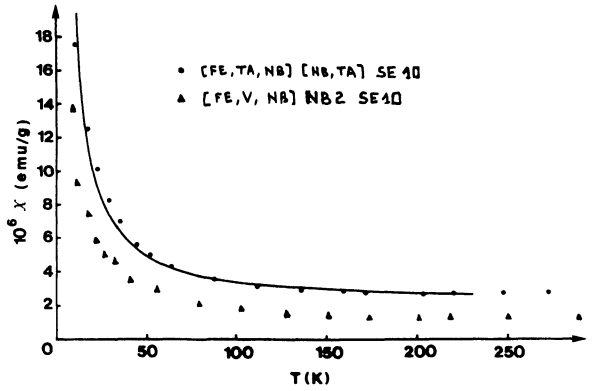

Fig. 7. — Magnetic susceptibility *versus* temperature for the (Fe, V)Nb_2Se_{10} and (Fe, Ta)Nb_2Se_{10}. The solid line is calculated from the equation given by Kobayashi *et al.* [8] which represents the susceptibility of localized states with U = 240 K for (Fe, Ta)Nb_2Se_{10}.

the Pauli like paramagnetism while the temperature dependent part can be expressed, within a limited temperature range, by the Curie-Weiss formula

$$\chi = \frac{C}{T - \theta} + \chi_0 \cdot$$

After correction for the ion core diamagnetism, the minimum values of the susceptibilities are given in table VI.

If these values are assumed to correspond to the Pauli paramagnetism without exchange enhancement, the density of states at the Fermi level is given as 28.9/eV.mole.spin for (Fe, V, Nb)N_2Se_{10}, 58.9/eV.mole.spin for (Fe, Ta, Nb) (Nb, Ta)Se_{10} and

Table VI. — *The minimum values of the susceptibility after correction for the ion-core diamagnetism.*

	χ_p^o (emu,mole^{-1})
(Fe,V,Nb)Nb_2Se_{10}	$1.73\ 10^{-3}$
(Fe,Ta,Nb)(Ta,Nb)Se_{10}	$3.81\ 10^{-3}$
(Fe,Nb)Nb_2Se_{10}	$2.26\ 10^{-3}$

Correction for the ion-core diamagnetism according to Klemm :

Fe^{2+} ($-$ 13 $\times$ 10^{-6} emu/mole);
V^{3+} ($-$ 10 $\times$ 10^{-6} emu/mole);
Nb^{4+} ($-$ 16 $\times$ 10^{-6} emu/mole);
Se^{2-} ($-$ 48 $\times$ 10^{-6} emu/mole)

and

Ta^{4+} ($-$ 23 $\times$ 10^{-6} emu/mole).

35/eV.mole.spin for (Fe, Nb)Nb_2Se_{10}. It is clear that these values are too large for normal metals. The density of state $D(E)$ is given by

$$D(E) \equiv \frac{dN}{dE} = \frac{dN}{dk}\frac{dk}{dE} = \frac{dN}{dk}\left(\frac{dE}{dk}\right)^{-1}.$$

In a purely one dimensional free electron system, $\frac{dN}{dk} = \frac{2a}{\pi}\sqrt[3]{N}.\frac{dE}{dk}$ may be estimated from the $E(k)$ curve calculated by Whangbo *et al.* [4] who made band structure calculations of $FeNb_3Se_{10}$. From their result the density of states is estimated as of the order of 1. The value $D(E_F)$ = 1/eV.mole.spin, was obtained assuming $dE/dk = 0$ [4]. So, there is an assumption and an approximation. This value differs largely from the above ones. This could be related to the fact that we neglected any interaction between conduction electrons. Taking into account an interaction allows us to replace the former relation $\chi_\rho = 2\,D(E_F)\,\mu_B^2$ (for one spin direction) by :

$$\chi_p = \frac{\chi_\rho^0}{1 - D(E_F)\,V_c}, \text{ where } V_c \text{ is referred to the interaction.}$$

With the $FeNb_3Se_{10}$ example, we find a large value $D(E_F)\,V_c \sim 0.97$ which has the same order of magnitude as that of the nearly ferromagnetic metal Pd. As our samples are not ferromagnetics, the disagreement between the values of density of states cannot be attributed to the fact that interactions have been neglected.

In the preceding section, we discussed the large increase of the resistivity as due to Anderson localization in the C.D.W. state. Each Anderson localized state is occupied by a single electron as far as it is near the Fermi level, due to the Coulomb interaction between electrons in the same state. States far below the Fermi surface are occupied by two electrons and are non-magnetic. The magnetic susceptibility of the Anderson localized states system was calculated by Kobayashi *et al.* [8] as

$$\chi = \frac{N(0)\,\mu_B \sinh \beta\mu_B H}{H\beta(\cosh^2 \beta\mu_B H - e^{-\beta U})^{1/2}} \cdot \times$$

$$\times \operatorname{Ln} \frac{\cosh \beta\mu_B H + (\cosh^2 \beta\mu_B H - e^{-\beta U})^{1/2}}{\cosh \beta\mu_B H - (\cosh^2 \beta\mu_B H - e^{-\beta U})^{1/2}}.$$

Where $N(0)$ is the density of localized states, $\beta = (k_B T)^{-1}$, and U is the effective Coulomb interaction between electrons in the same state. A comparison with the experimental result is shown in figure 7. As evident from the figure, a value of U of the order of 240 K can reproduce the experimental data. The high temperature value corresponds to $2\,N(0)\,\mu_B^2$. The susceptibility calculated from the above formula is nearly field-independent as long as $\mu_B H \sim 1$ K ($H \sim 10^4$ Oe), that is also consistent with the experi-

mental finding. The best choice of U is (240 ± 20 K) for all the three compounds, which have the same structure. Assuming that the density of states is constant, the number of localized states contributing to the susceptibility is 1.2 per chemical formula for $FeTaNb_2Se_{10}$ and 0.6 for $FeVNb_2Se_{10}$. It is interesting that $FeVNb_2Se_{10}$ which exhibits a resistivity rise in the weakly localized regime has the smallest value of number of states.

In short, the weak-field susceptibility can be explained as due to Anderson localized states, along with the electrical resistivity.

Note added in proof. — Recently measurements on similar compounds have been reported by Cava *et al.* *Phys. Rev. B* **27** (1983) 7412.

Acknowledgments.

We would like to thank P. Monceau (C.R.T.B.T.-C.N.R.S. Grenoble) for useful discussions and comments.

References

[1] HILLENIUS, S. J. and COLEMAN, R. V., *Phys. Rev. B* **25** (4) (1982) 2191.

[2] CAVA, R. J., HIMES, V. L., MIGHELL, A. D. and ROTH, R. S., *Phys. Rev. B* **24** (6) (1981) 3634.

[3] MEERSCHAUT, A., GRESSIER, P., GUEMAS, L. and ROUXEL, J., *Mat. Res. Bull.* **16** (1981) 1035.

[4] WHANGBO, M. H., CAVA, R. J., DISALVO, F. J. and FLEMING, R. M., *Solid State Commun.* **43** (1982) 277.

[5] BEN SALEM, A., MEERSCHAUT, A., GUEMAS, L. and ROUXEL, J., *Mat. Res. Bull.* **17** (1982) 1071.

[6] HILLENIUS, S. J., COLEMAN, R. V., FLEMING, R. M. and CAVA, R. J., *Phys. Rev. B.* **23** (4) (1981) 1567.

[7] MORET, R., POUGET, J. P., MEERSCHAUT, A. and GUEMAS, L., *J. Physique Lettres* **44** (1983) L-93.

[8] KOBAYASHI, S., FUNAGAWA, Y., IKEHATA, S. and SASAKI, W., *J. Phys. Soc. Jpn* **45** (1978) 1276.

[9] LEE, P. A., RICE, T. M. and ANDERSON, P. W., *Phys. Rev. Lett.* **31** (1973) 462.

[10] ETEMAD, S., *Phys. Rev. B* **13** (1976) 2254.

[11] WANG, Z. Z., MONCEAU, P., RENARD, M., GRESSIER, P., GUEMAS, L. and MEERSCHAUT, A., *Solid State Commun.* **47** (1983) 439.

[12] MOTT, N., PEPPER, M., POLLITT, S., WALLIS, R. H. and ADKINS, C. T., *Proc. R. Soc. London A* **345** (1975) 169.